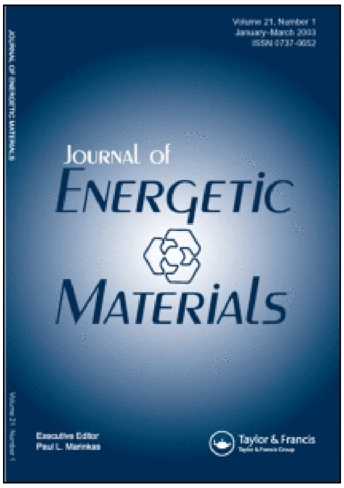

Journal of Energetic Materials
Publication details, including instructions for authors and subscription information:
http://www.informaworld.com/smpp/title~content=t713770432

Effect of Initial Temperature and Pressure on the Burning Rate of AGAT/AN Mixtures

Yasuyoshi Miyata[a]; Kazuo Hasue[a]
[a] Department of Applied Chemistry, National Defense Academy, Kanagawa, Japan

To cite this Article Miyata, Yasuyoshi and Hasue, Kazuo(2011) 'Effect of Initial Temperature and Pressure on the Burning Rate of AGAT/AN Mixtures', Journal of Energetic Materials, 29: 1, 26 — 45
To link to this Article: DOI: 10.1080/07370652.2010.498778
URL: http://dx.doi.org/10.1080/07370652.2010.498778

Journal of Energetic Materials, 29: 26–45, 2011

ISSN: 0737-0652 print/1545-8822 online
DOI: 10.1080/07370652.2010.498778

Effect of Initial Temperature and Pressure on the Burning Rate of AGAT/AN Mixtures

YASUYOSHI MIYATA and
KAZUO HASUE

Department of Applied Chemistry, National Defense
Academy, Kanagawa, Japan

The combustion characteristics of aminoguanidinium 5,5′-azobis-1H-tetrazolate (AGAT)/ammonium nitrate (AN)-based gas generating agents were studied by using a temperature-controlled chimney-type strand burner. Controlling the initial temperature at 243, 298, or 343 K, the mass burning rates of AGAT/AN = 50/50 were measured and the temperature sensitivities were deduced. The effects of CuO and MnO_2 on temperature sensitivity were studied. The temperature sensitivity equation as a function of pressure and initial temperature was also determined.

Keywords: AGAT, ammonium nitrate, mass burning rate, temperature sensitivity

Introduction

It is desirable for an air bag to maintain its time required for inflation regardless of low temperature in winter and high temperature in summer. If the burning rate of the gas-generating agents becomes too fast under high temperature conditions, an air bag would inflate too rapidly, causing injury or even

Address correspondence to Kazuo Hasue, Department of Applied Chemistry, National Defense Academy, Hashirimizu 1-10-20, Yokosuka, Kanagawa 239-8686, Japan. E-mail: hasue@nda.ac.jp

death of a passenger, and if the burning rate becomes too slow under low temperature conditions, it would be impossible to protect the passenger.

If the temperature sensitivity of the burning rate is large, the rate of inflation of an air bag would change with a change in temperature, which is undesirable for an air bag used under fluctuating temperature conditions, so it is desirable for the temperature sensitivity to be small.

Factors that affect the burning rate of the propellants are pressure and temperature, and there has been much research on the effect of initial temperature on the burning rate of rocket propellants [1–9] but there does not seem to be such research related to air bag gas-generating agents.

Ammonium nitrate (AN) has been attracting attention as an oxidizer of clean gas-generating mixtures. However, the gas-generating mixtures that contain AN have the disadvantages that they are difficult to ignite and the burning rate is generally slow.

The authors have focused attention on the reactivity of aminoguanidinium 5,5′-azobis-1H-tetrazolate (AGAT) and have conducted research to develop air bag gas-generating mixtures using AGAT-based mixtures with strontium nitrate [10], copper(II) nitrate [11], and AN [12]. It was reported that, based on the burning test of AGAT/AN mixtures, AGAT is promising as a fuel of AN [12]. In this study, the effect of initial temperature and pressure on the burning rate of AGAT/AN mixtures was studied.

Experimental

Materials

AGAT (Toyo Kasei Kogyo Co., Ltd., Tokyo, Japan), which is sold commercially as ABAG, was sieved through Japanese Industrial Standards (JIS) sieves and dried at 333 K for 24 hr in a vacuum drying oven. Particle size range of 45–75 μm was used. After AN (Kanto Chemical Co., Inc., Tokyo, Japan, JIS special grade reagent) was milled using a vibration ball mill, it was dried at 333 K for 24 hr in a vacuum drying oven and sieved through JIS standard sieves. Particle size range of 150–300 μm was used. CuO (Kanto Chemical Co., Inc., Kanto extra pure grade reagent) of the average particle size of 3.3 µm and MnO_2 (Kanto Chemical Co., Inc., Kanto extra pure grade reagent) of the average particle size of 53.9 µm were used. Fuel particles and oxidizer particles were mixed at a designated mixing ratio for 30 min at 80 rpm in a rotary mixer (S-3, Tsutsui Scientific Instruments Co., Ltd., Tokyo, Japan). The compositions used in this study are given in Table 1.

Instrumentation

One and a half grams of AGAT/AN mixtures was compressed at approximately 300 MPa for 5 min to make columnar samples. The sides of columnar samples were coated with epoxy resin to assure cigarette burning. A combustion test was performed by using a pressure- and temperature-controlled chimney-type strand burner with an optical window (TDK-15011, Tohata Denshi Co., Ltd., Tokyo, Japan) under approximately 2–6 MPa N_2 atmosphere at 243, 298, and 343 K. The ignition of the strand was carried out through a heated nichrome wire (diameter 0.6 mm). Pressure within the chamber P was measured using a strain-gauge pressure transducer (PG-100KU-F, Kyowa Electronic Instruments Co., Ltd., Tokyo, Japan) and after amplification through a signal amplifier (CDV-230C, Kyowa Electronic Instruments Co., Ltd.), the data were recorded on a digital data recorder (GR-3000, Keyence Corp., Osaka, Japan). The mass burning rate r_m was deduced from the endurance of

Table 1
Composition of gas-generating agents

	Parts by weight			
Sample	AGAT	AN	CuO	MnO_2
A	50	50	–	–
B	50	50	5	–
C	50	50	–	5

the recorded pressure rise. Pressure starts to rise as soon as the sample starts burning and the pressure stops rising when the burning ceases. Average internal pressure was calculated by averaging out the pressures at the start and end of combustion.

Results and Discussion

Effects of Initial Temperature and Catalysts on the Burning Rates

Figure 1 gives the relationship between P and r_m at a given initial temperature T_i with or without the addition of CuO. The mass burning rate r_m increases with an increase in pressure and obeys Vieille's law (Eq. (1)).

$$r_\mathrm{m} = \rho r = \rho a P^n = \mathrm{a_m} P^n \tag{1}$$

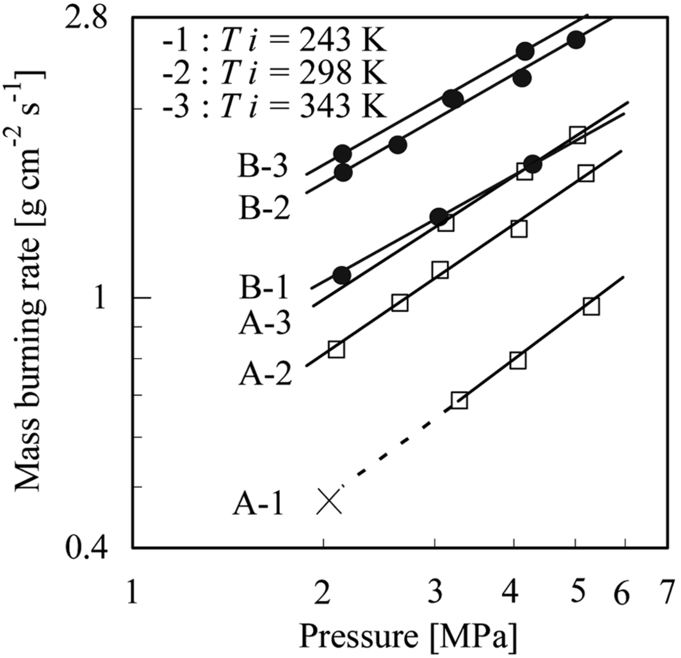

Figure 1. Effects of CuO on mass burning rate at 243, 298, and 343 K.

where ρ is density, r is linear burning rate, a and a_m are constants, and n is the pressure exponent of the burning rate.

Because CuO increases r_m at each temperature, it is clear that CuO acts as a positive catalyst for the burning rate of the AGAT/AN mixture at the temperature range between 243 an 343 K. The mass burning rate r_m increases with an increase in T_i regardless of the addition of CuO, probably because the burning reaction, which includes a gas-phase elementary reaction, is promoted with an increase in temperature. Burning interruption occurred at 243 K, 2 MPa for sample A, which does not contain a catalyst, probably because the AN decomposition ceases to occur at a low temperature.

Figure 2 shows the effect of T_i and the addition of MnO_2 on r_m. There was also an increase in r_m with an increase in T_i when MnO_2

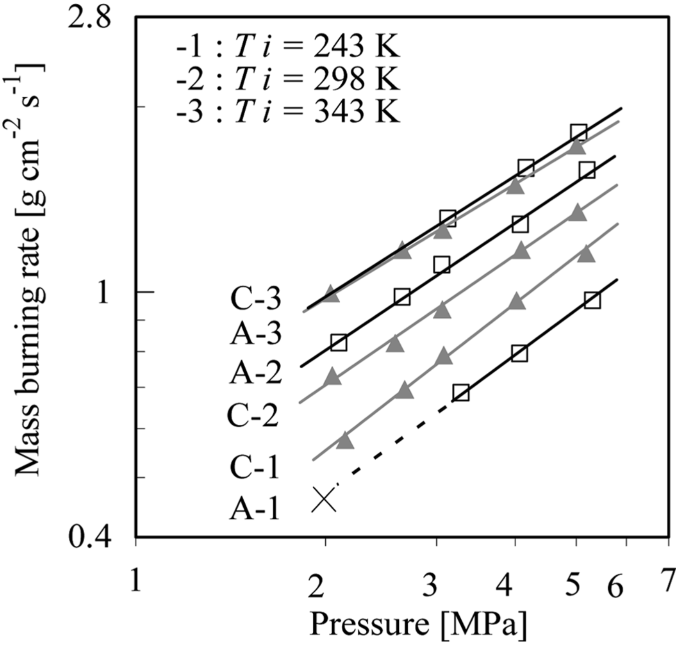

Figure 2. Effects of MnO_2 on mass burning rate at 243, 298, and 343 K.

was added, and it was shown that MnO_2 acts as a positive catalyst at 243 K, whereas it acts as a negative catalyst at 298 or 343 K.

The values of a_m and n are shown in Table 2. The pressure exponent n decreases with an increase in T_i. It was also found that, because n for the CuO-added sample becomes smaller than the n for the additive-free sample at each T_i, CuO has an effect of reducing n also. On the other hand, even though n for the MnO_2-added sample became smaller with an increase in T_i, n is smaller than that of the additive-free mixture only at 343 K.

Effect of Temperature and Pressure on Temperature Sensitivity

Assuming that the pressure is constant, the change in the burning rate with the change in temperature is defined as the temperature sensitivity σ_p, whose equation is as given in the following [13]:

$$\sigma_p = \frac{1}{r}\frac{\Delta r}{\Delta T_i} = \frac{1}{r}\left[\frac{\partial r}{\partial T_i}\right]_p = \left[\frac{\partial lnr}{\partial T_i}\right]_p \tag{2}$$

Here, p shows any pressure. Inserting $r \cdot \rho = r_m$ into the above equation,

$$\sigma_p = \frac{1}{r_m}\frac{\Delta r_m}{\Delta T_i} = \frac{1}{r_m}\left[\frac{\partial r_m}{\partial T_i}\right]_p = \left[\frac{\partial lnr_m}{\partial T_i}\right]_p \tag{3}$$

Table 2

Value of a_m and pressure exponent n for samples

Initial temperature (K)	a_m			n		
	Sample A	Sample B	Sample C	Sample A	Sample B	Sample C
243	0.292	0.696	0.318	0.719	0.588	0.792
298	0.499	1.03	0.434	0.694	0.565	0.701
343	0.612	1.10	0.643	0.672	0.563	0.611

Here, r_{mi} gives the mass burning rate at T_{i}. It is a function of temperature T_{i} because it changes with ambient temperature T. The relationshp between r_{mi} and T_{i} for each mixture is given in Figs. 3–5. In each situation, the burning rate increases with an increase in T_{i}. Because the relations between r_{mi} and T_{i} could be approximated by a curve, a second-order equation as a function of T_{i} [1] was employed in this study.

$$r_{\mathrm{mi}} = b_2(p)T_{\mathrm{i}}^2 + b_1(p)T_{\mathrm{i}} + b_0(p) \tag{4}$$

The relations between σ_{p} and pressure for each sample calculated at 243, 268, 293, 318, and 343 K are shown in Figs. 6–8.

The following tendencies could be seen regarding the relation between σ_{p} and pressure for AGAT/AN/additive mixtures. σ_{p} decreases with an increase in pressure for each mixture at T_{i} between 243 and 343 K. Although the rate of decrease in σ_{p} is almost constant regardless of T_{i} for the additive-free mixture and CuO-added mixture, that of the MnO_2-added mixture is

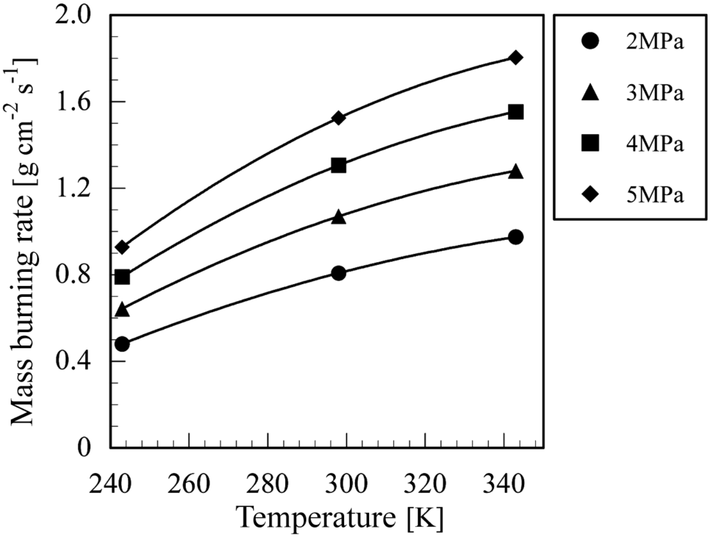

Figure 3. Mass burning rate vs. temperature for sample A.

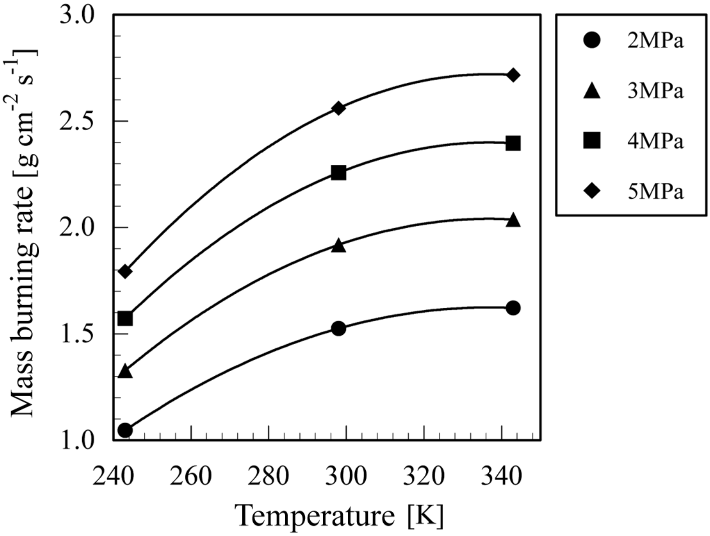

Figure 4. Mass burning rate vs. temperature for sample B.

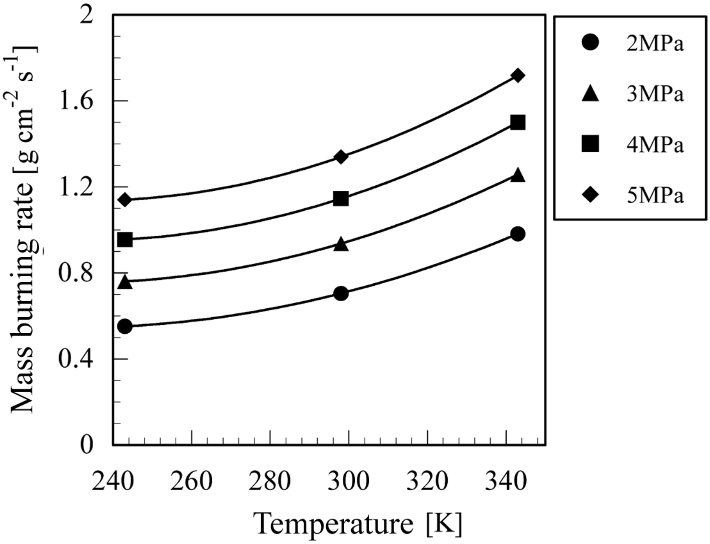

Figure 5. Mass burning rate vs. temperature for sample C.

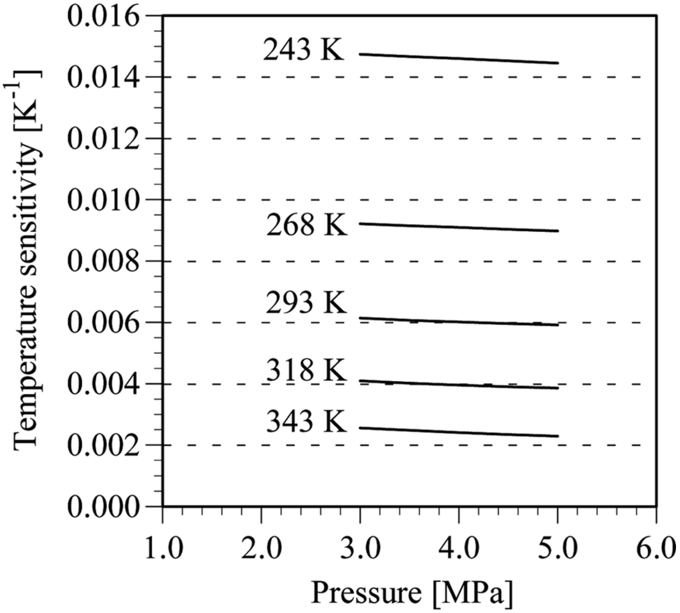

Figure 6. Temperature sensitivity of burning rate vs. pressure for sample A.

larger. σ_p increases with a decrease in T_i for additive-free and CuO-added mixtures, whereas it increases with an increase in T_i for the MnO_2-added mixture. σ_p decreases with an increase in pressure and T_i for the additive-free mixture and CuO-added mixture, whereas it decreases with an increase in pressure and a decrease in T_i for the MnO_2-added mixture. Addition of CuO decreases σ_p compared with the additive-free mixture. Addition of MnO_2 decreases the temperature sensitivity but it increases with an increase in temperature.

If the burning rate increases under high temperature, the rate of inflation of an air bag would change with a change in temperature, which is undesirable for an air bag. Therefore, CuO would be an effective additive, increasing the burning rate while decreasing the temperature sensitivity under high temperature.

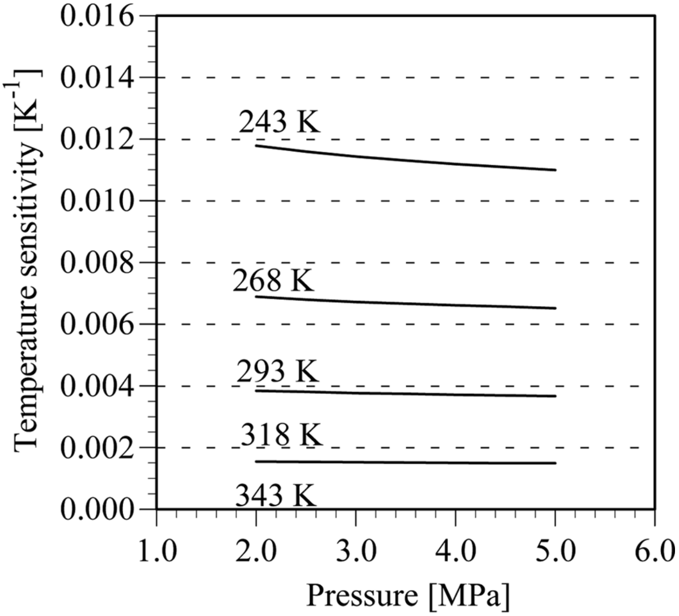

Figure 7. Temperature sensitivity of burning rate vs. pressure for sample B.

Theoretical Analysis of Temperature Sensitivity

Theoretical studies have been carried out over the years on the mechanisms regarding temperature sensitivity [2–4]. According to Kubota and Ishihara [2], temperature sensitivity could be divided into temperature sensitivity of gas-phase reactions and temperature sensitivity of condensed-phase reactions, and these can be examined if gas-phase and condensed-phase reactions are understood in detail. There have also been elementary studies by Glick [3] and Cohen and Flanigan [4].

A schematic diagram of the energy balance of a combustion wave is given in Fig. 9. Balancing out the heat energy equation near the burning surface, assuming a steady burning state, the following equation is derived:

$$Q_1 + Q_2 = Q_3 \tag{5}$$

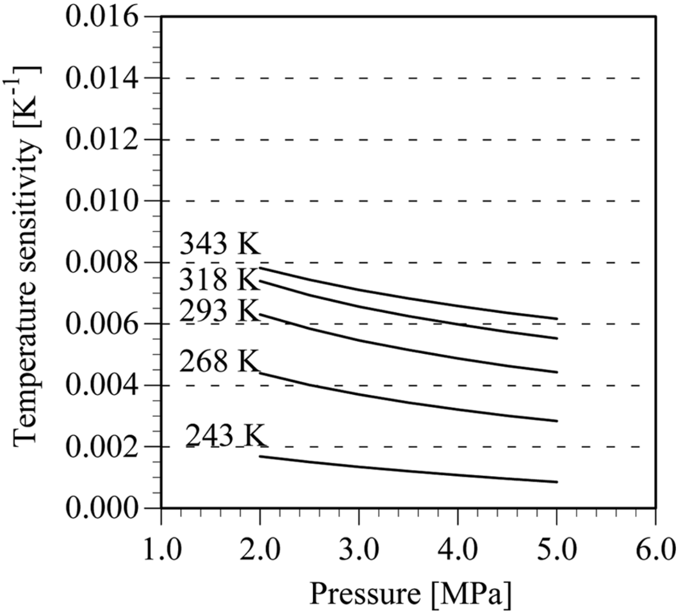

Figure 8. Temperature sensitivity of burning rate vs. pressure for sample C.

Here, Q_1 (J m^{-2} s^{-1}) is the amount of heat transfer per unit area and unit time from the gas phase to the burning surface, Q_2 (J m^{-2} s^{-1}) is the amount of heat release per unit area and unit time from the condensed phase, and Q_3 (J m^{-2} s^{-1}) is the amount of heat transfer per unit area and unit time to the unburned region in the solid phase, which can be expressed by the following equations:

$$Q_1 = \lambda_{\mathrm{g}}(dT/dx)_{\mathrm{g}} \tag{6}$$

$$Q_2 = \rho r Q_{\mathrm{s}} \tag{7}$$

$$Q_3 = \rho C_{\mathrm{p}} r(T_{\mathrm{s}} - T_{\mathrm{i}}) \tag{8}$$

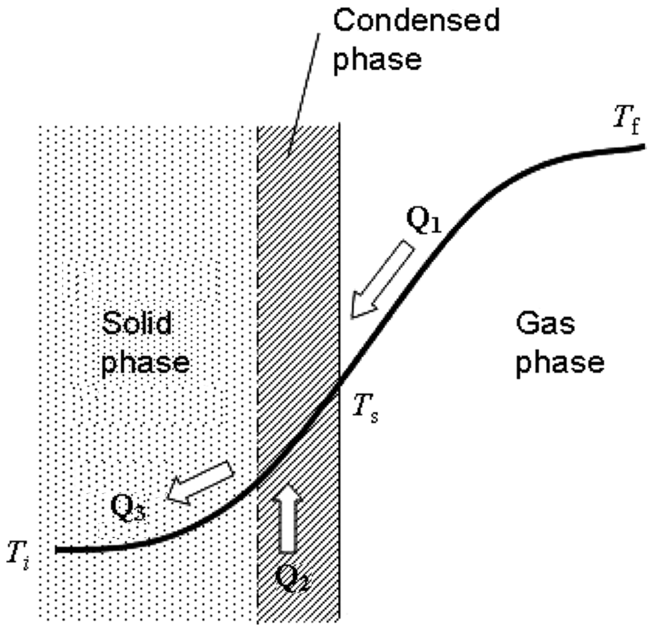

Figure 9. Energy balance near the burning surface.

Here, Q_s (J g^{-1}) is the amount of heat generation per unit mass at the condensed phase and C_p is the specific heat (J K^{-1} g^{-1}).

Substitution of Eq. (5) into Eqs. (6)–(8) followed by simplification gives the following equation:

$$r = \frac{\lambda_g (dT/dx)_g}{\rho C_p (T_s - T_i - Q_s/C_p)} \tag{9}$$

Taking the natural log of both sides of Eq. (9) and then differentiating by T_i gives the following equation:

$$\sigma_p = \left(\frac{\partial \ln \phi_g}{\partial T_i}\right)_p - \left(\frac{\partial \ln \psi}{\partial T_i}\right)_p \tag{10}$$

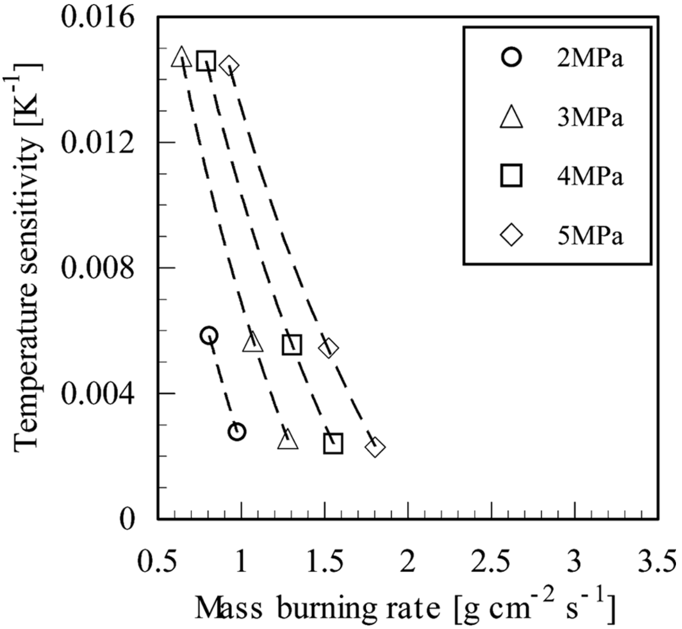

Figure 10. Temperature sensitivity vs. mass burning rate for sample A.

where $\phi_g = (dT/dx)_g$ is the temperature gradient at the gas phase, and $\psi = T_s - T_i - Q_s/C_p$. In addition, if we assume that

$$\phi = (\partial ln\phi_g/\partial T_i)_p \tag{11}$$

$$\psi = -(\partial ln\psi/\partial T_i)_p \tag{12}$$

σ_p becomes

$$\sigma_p = \phi + \psi \tag{13}$$

where ϕ is the temperature sensitivity in the gas phase and ψ is the temperature sensitivity in the condensed phase [13]. Assuming that ϕ_g is not affected by T_i, that is, ψ is dominating,

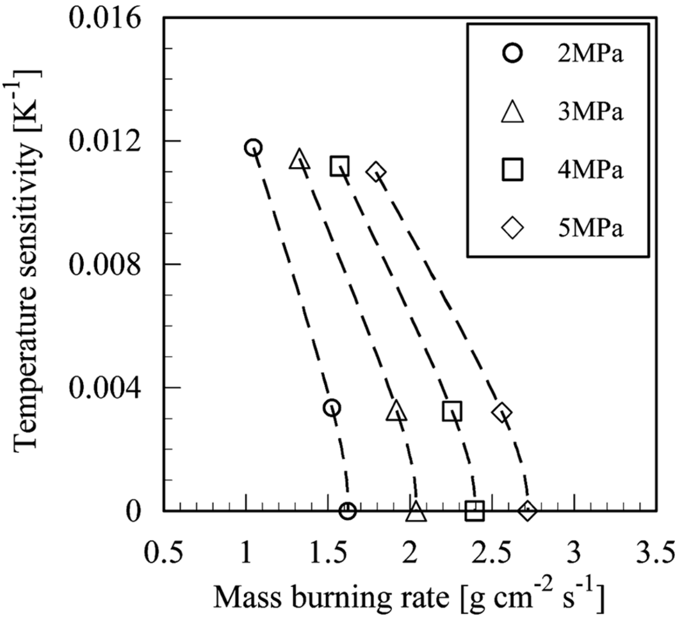

Figure 11. Temperature sensitivity vs. mass burning rate for sample B.

$\phi \approx 0$, hence,

$$\sigma_p = \psi = \frac{1 - (\partial T_s/\partial T_i)_p}{T_s - T_i - Q_s/C_p} \tag{14}$$

In addition, because T_s is virtually not affected by T_i, $(\partial T_s/\partial T_i)_p$ is approximately 0. Therefore, σ_p when the temperature sensitivity in the condensed phase is dominating can be expressed by the following equation:

$$\sigma_p = \frac{1}{T_s - T_i - Q_s/C_p} \tag{15}$$

When pressure increases at a given T_i, T_i increases due to boiling point elevation. Q_s and C_p remain constant because

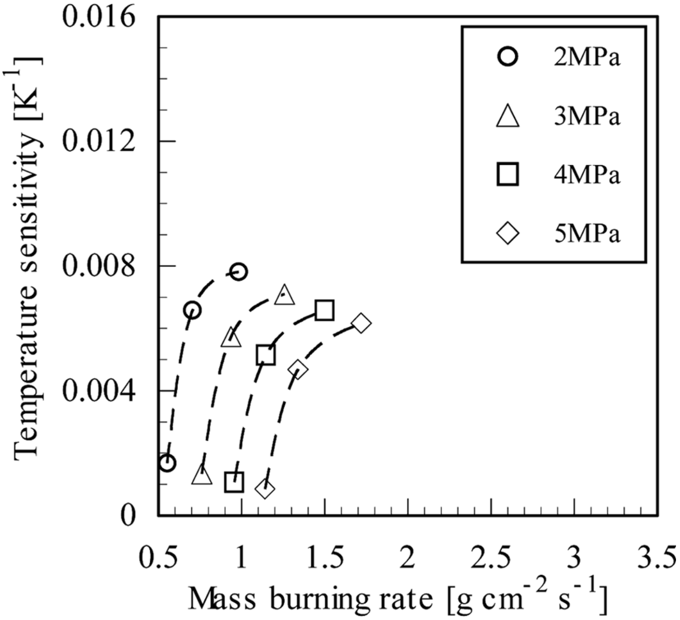

Figure 12. Temperature sensitivity vs. mass burning rate for sample C.

they depend on the materials that form the system. Hence, according to Eq. (15), σ_p decreases with an increase in pressure when the temperature sensitivity in the condensed phase is dominating. Therefore, because σ_p generally decreases with an increase in temperature regardless of the addition of CuO or MnO_2, according to Figs. 6–8, it could be said that σ_p for AGAT/AN mixtures at 243–343 K is governed by the temperature sensitivity in the condensed phase.

In situations where σ_p decreases with an increase in pressure and the temperature sensitivity in the condensed phase becomes dominant, there is a tendency of the existence of a relatively thick condensed phase [14,15], similar to that in this study. In contrast, in situations where σ_p increases with an increase in pressure, the temperature sensitivity in the gas phase is generally dominant, and there is a tendency of the

Table 3
Values of K_0, K_1, K_2, K_3, K_4, K_5, K_6, and K_7

Sample	A	B	C
K_0	3.9549681×10^{-1}	4.2204189×10^{-1}	$-1.3079799 \times 10^{-1}$
K_1	$-3.4738045 \times 10^{-3}$	$-3.8846852 \times 10^{-3}$	1.0534557×10^{-3}
K_2	1.0442960×10^{-5}	1.2260864×10^{-5}	$-2.5363634 \times 10^{-6}$
K_3	$-1.0640000 \times 10^{-8}$	$-1.3216000 \times 10^{-8}$	1.9146667×10^{-9}
K_4	3.8573690	-2.1696631	-2.5557427×10
K_5	$-4.4328253 \times 10^{-2}$	2.1294152×10^{-2}	2.3864047×10^{-1}
K_6	1.6957368×10^{-4}	$-7.2432320 \times 10^{-5}$	$-7.5820960 \times 10^{-4}$
K_7	$-2.1850667 \times 10^{-7}$	8.3413333×10^{-8}	8.0906667×10^{-7}

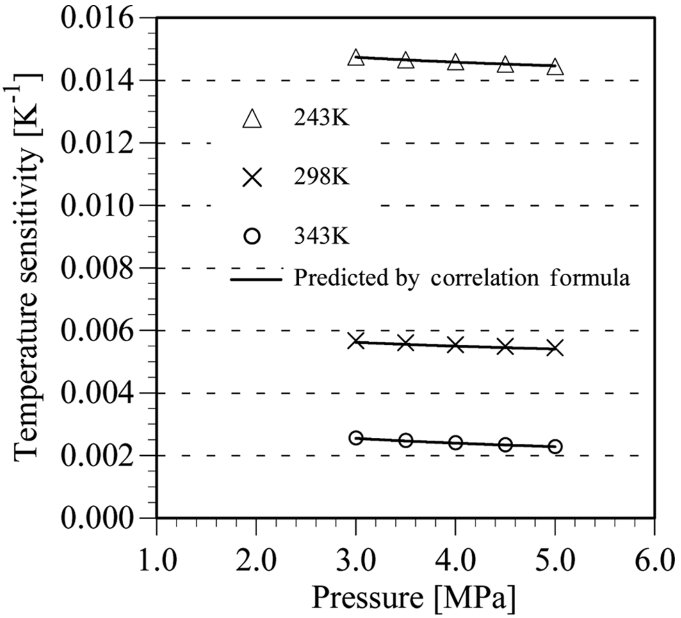

Figure 13. Correlation of temperature sensitivity with pressure and initial temperature for sample A.

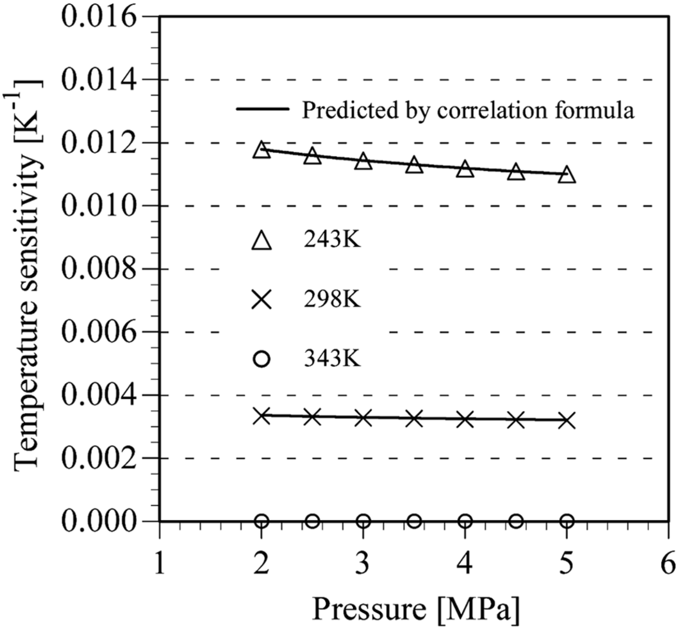

Figure 14. Correlation of temperature sensitivity with pressure and initial temperature for sample B.

nonexistent condensed phase, as in the mixture that uses AP as an oxidizer [15].

Relation between Temperature Sensitivity and Burning Rate

Figures 10–12 show the relation between σ_p and r_m at each pressure. The tendency is clear such that, as r_m increases with an increase in T_i, σ_p for the original mixture or CuO-added mixture decreases, whereas σ_p for the MnO_2-added mixture increases.

Equation of Temperature Sensitivity as a Function of Pressure and Temperature

The relations between σ_p and vessel pressure, together with the relation between σ_p and temperature, were investigated according to Figs. 6–8. These equations could be expressed as given in the following equations [14]:

$$\sigma_{\mathrm{p}} = (K_0 + K_1 T_{\mathrm{i}} + K_2 T_{\mathrm{i}}^2 + K_3 T_i^3) P^{\kappa} \tag{16}$$

$$\kappa = (K_4 + K_5 T_{\mathrm{i}} + K_6 T_{\mathrm{i}}^2 + K_7 T_{\mathrm{i}}^3) \tag{17}$$

The calculated coefficients K_0–K_7 are given in Table 3. The units of T_{i}, P, and σ_{p} are K, MPa, and K^{-1}, respectively. Figures 13–15 show the results derived from Eqs. (15) and (16). These data agreed well under wide ranges of ambient temperature and pressure. It can be said that Eqs. (15) and (16) are useful in not only the theoretical analysis of r_{m} but also in designing mixtures [14].

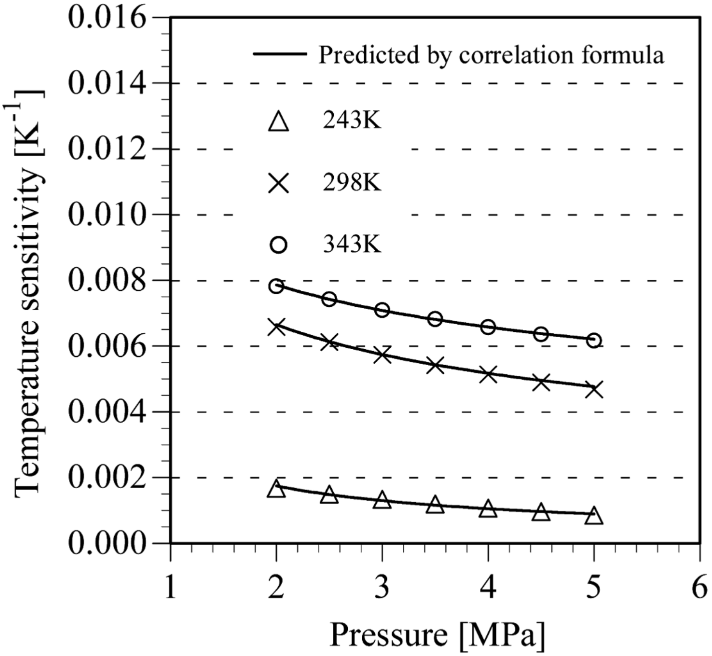

Figure 15. Correlation of temperature sensitivity with pressure and initial temperature for sample C.

Conclusion

The burning rates for AGAT/AN mixtures, together with CuO- or MnO_2-added mixtures, at different initial temperatures were measured and the following conclusions were drawn.

Mass burning rate for each mixture increases with an increase in initial temperature.

Within the temperature range tested, temperature sensitivity decreases with an increase in pressure.

Temperature sensitivities for the additive-free mixture and CuO-added mixture decrease with an increase in initial temperature or burning rate, whereas temperature sensitivity for the MnO_2-added mixture increases.

The contributions of the gas phase and the solid phase were investigated and it was found that the temperature sensitivity at the condensed phase plays a dominant role.

CuO increases the burning rate and decreases the temperature sensitivity at high temperature; therefore, it would probably be an effective additive.

References

[1] Yang, A. S., I. H. Huang, W. H. Hsieh, and K. K. Kuo. 1993. Burning-rate characteristics of boron/[BAMO/NMMO] fuel-rich solid propellant under broad ranges of pressure and temperature. In K. K. Kuo and R. Pein (ed.), *Combustion of Boron-Based Solid Propellants and Solid Fuels*, Boca Raton, FL: CRC Press.

[2] Kubota, N. and A. Ishihara. 1984. Analysis of the temperature sensitivity of double-base propellants. In *Proceedings of the 20th Symposium (International) on Combustion*, Pittsburgh, PA: The Combustion Inst.

[3] Glick, R. L. 1967. Temperature sensitivity of solid propellant burning rate. *American Institute of Aeronautics and Astronautics*, 5: 586–587.

[4] Cohen, N. S. and D. A. Flanigan. 1985. Mechanisms and models of solid-propellant burn rate temperature sensitivity: A review. *American Institute of Aeronautics and Astronautics*, 23: 1538–1547.

[5] Salizzoni, R. M., W. H. Hsieh, and K. K. Kuo. 1993. Temperature sensitivity measurements and regression behavior of a

family of boron-based very high burning rate propellants. In K. K. Kuo and R. Pein (ed.), *Combustion of Boron-Based Solid Propellants and Solid Fuels*, Boca Raton, FL: CRC Press.

[6] Kubota, N. and S. Miyazaki, 1987. Temperature sensitivity of burning rate of ammonium perchlorate propellants. *Propellants, Explosives, Pyrotechnics*, 12: 183–187.

[7] Kulkarni, V. V., A. R. Kulkarni, P. A. Phawade, and J. P. Agrawal. 2001. A study on the effect of additives on temperature sensitivity in composite propellants. *Propellants, Explosives, Pyrotechnics*, 26: 125–129.

[8] Judge, M. D. and P. Lessard. 2007. An advanced GAP/AN/TAGN propellant. Part I: Ballistic properties. *Propellants, Explosives, Pyrotechnics*, 32: 175–181.

[9] Cauty, T. J., Cl. Demarais, and Ch. Erades. 1993. Determination of solid propellant burning rate sensitivity to the initial temperature by the ultrasonic method. In K. K. Kuo and R. Pein (ed.) *Combustion of Boron-Based Solid Propellants and Solid Fuels*, Boca Raton, FL: CRC Press.

[10] Iwakuma, K., Y. Miyata, S. Date, M. Kohga, and K. Hasue. 2007. A study on the combustion of 5,5′-azobis-tetrazole aminoguanidine/strontium nitrate as a gas generating agent. *Science and Technology of Energetic Materials*, 68(4): 95–101.

[11] Miyata, Y., K. Morita, K. Iwakuma, M. Abe, S. Date, and K. Hasue. 2007. Burning characteristics of the consolidated mixtures of aminoguanidium 5,5′-azobis-tetrazolate and copper(II) oxide. *Science and Technology of Energetic Materials*, 68(6): 153–159.

[12] Miyata, Y. M. Abe, S. Date, M. Kohga, and K. Hasue. 2008. Burning characteristics of aminoguanidinium 5,5′-azobis-tetrazolate/ammonium nitrate as gas penetrating mixtures. *Science and Technology of Energetic Materials*, 69(4): 117–122.

[13] Kubota, N. 2007. *Propellants and Explosives*. Weinheim: Wiley-VCH Verlag.

[14] Sinditski, V. P., V. Y. Egorshev, A. I. Levshenkov, and V. V. Serushkin. 2006. Combustion of ammonium dinitramide, Part 1: Burning behavior. *Journal of Propulsion and Power*, 22: 769–775.

[15] Atwood, A. I., T. L. Boggs, P. O. Curran, T. P. Parr, and D. M. Hanson-Parr. 1999. Burning rate of solid propellant ingredients, Part 2: Determination of burning rate temperature sensitivity. *Journal of Propulsion and Power*, 15: 748–752.